RSC Advances

ROYAL SOCIETY OF CHEMISTRY

www.rsc.org/advances

Chiral ionic liquid crystals with a bulky rigid core from renewable camphorsulfonic acid

Xiaoping Rao,[a,b,c] Jinwen Zhang,*[b] Jianqiang Zheng,[a] Zhanqian Song[a] and Shibin Shang[a]

[a] Institute of Chemical Industry of Forestry Products, CAF; Key Lab. of Biomass Energy and Material, Jiangsu Province; National Engineering Lab. for Biomass Chemical Utilization; Key and Lab. on Forest Chemical Engineering, SFA, Nanjing 210042, China. Fax: + 86 25-85413445; Tel: + 86-25-85482452; E-mail: rxping2001@163.com

[b] School of Mechanical and Materials Engineering, Composite Materials and Engineering Center, Washington State University, Pullman, WA, 99164, USA. Fax: +1 509-335-5077; Tel: +1 509-335-8723; E-mail: jwzhang@wsu.edu

[c] Institute of Forest New Technology, CAF, Beijing 100091, PR China

* To whom correspondence should be addressed. Tel.: 509-335-8723; Fax: 509-335-5077; E-mail: jwzhang@wsu.edu.

Abstract

Renewable chiral bulky rigid D- and L-camphorsulfonic acids were introduced as new building blocks in the design of ionic liquid crystals with long chain alkylamines ($C_nH_{2n+1}NH_2$; n = 12, 14, 16 and 18) by the direct reaction of acid and amine. The phase transition behaviors of the obtained salts were investigated using DSC, POM, FTIR, XRD and CD spectroscopy, respectively. The salts with shorter alkyl chain lengths exhibited lower liquid crystal transition temperatures and wider mesophase ranges. The vibration of the N-H bonds was weakened or even disappeared with increasing temperature, which was probably due to the decrease in the change of dipole moment of the liquid crystals.

Keywords: ionic liquid crystal; renewable; bulky rigid core; camphorsulfonic acid; SmB* phase

Introduction

Liquid crystal is usually regarded as the fourth state of matter between anisotropic solid and isotropic liquid.[1-3] A liquid crystal is thermotropic if it passes through different phases from solid to liquid on heating.[4] Recently, ionic liquid crystals (ILCs), which are composed of salts of cations and their counterpart anions, have attracted considerable attention in the areas of green chemical synthesis, separation, and nanomaterials synthesis because of low vapor pressure, high thermal stability, tunable polarity, easy recycling and a wide electrochemical window.[5-9] ILCs can be considered as materials combining properties of ionic liquids and liquid crystals. There are many kinds of ILCs including the widely studied ammonium, phosphonium, imidazolium, pyrrolidinium and pyridinium salts.[10-16] Since the discovery of liquid crystal (LC) state on cholesteryl-benzoate, the interest in the design and synthesis of chiral liquid crystal materials has been growing. Optical activity has been found to have a special effect on the liquid crystalline behavior, which sometimes leads to the formation of additional liquid crystal phases.[17-20]

In liquid crystals, mesophase results from a proper combination of the shape of a molecule and the magnitude and direction of interactions between molecules.[21] As recently reported, bulky rigid moiety is an important factor to induce and stabilize the mesophase, and rigid cores are known to have the ability to enhance the thermal stability of organic molecules.[22] Various rigid core structures, such as benzenesulfonic acid, pyridine-3-sulfonic acid, naphthalene sulfonic acid, hydroxyl nathalene sulfonic acid[23] and pyroglutamic acid[24], with long chain alkylamines can form thermotropic liquid crystals (LCs). However, the salts of naphthalene sulfonic acid and long chain alkylamine only exhibits a mesophase range of 30 ºC.[23] Long chain derivatives of guanine and

cytosine or their equimolar mixtures are also liquid-crystaline.[25]

Camphorsulfonic acid (CSA) has a rigid bulky bicyclic structure. It is obtained by sulfonation of camphor with sulfuric acid and acetic anhydride. Camphor is a natural chemical found in wood of the camphor laurel (*Cinnamomum camphora*). Camphor can also be prepared by multiple steps from α-pinene, [26] which is the main component of turpentine collected from the excludate of pine trees. Lyotropic liquid crystaline order has been observed in CSA dopped polyaniline (PANI) in *m*-cresol solution above a critical concentration, and this crystaline solution is useful for preparation oriented fibers and films with enhanced electrical and mechanical properties.[27] The bulky rigid and chirality characteristics of CSA intriggle us to investigate its thermotropic ionic liquid crystaline derivatives.

In this study, novel chiral ILCs, the alkylammonium salts of the bulky rigid D- and L-camphorsulfonic acids (D- and L-C_nACS), were prepared, (**Scheme 1**). The fatty chain length of the alkylamine (n) varied from 12 to 18 carbons. The objective of this study was to determine the effects of bulky rigid core, chirality, chain length of the tails on the liquid crystalline properties of alkylammonium camphorsulfonates. To the best of our knowledge, similar thermotropic ILCs using camphor as a building block has not been reported elsewhere. The liquid crystalline properties were investigated by differential scanning calorimetry (DSC), optical polarizing microscopy (OPM), variable temperature infrared (FTIR), variable temperature X-ray diffraction (XRD) and circular dichroism (CD) spectroscopy.

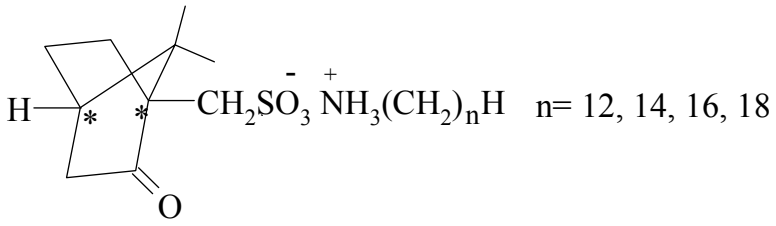

D- and L-C_nACS

Scheme 1. Structures of chiral D- and L-C_nACS ionic liquid crystals.

Experimental Section

D- and L-C_nACS were prepared by dissolving equimolar D- or L-camphorsulfonic acid and alkylamine in ethanol and allowing them to react at the reflux temperature for 4 h. The precipitated salts were filtered and recrystallized from ethanol, and the yields varied from 45 to 85% with the salts with longer alkyl chains being more easily to crystallize and having higher yields. The chemical structures of the salts were confirmed with ^{1}H NMR spectroscopy and elemental analysis. All reagents and solvents were of analytical grade and were used without further purification.

^{1}H-NMR spectra were recorded on a DPX-300 Bruker AVANCE 300 spectrometer using $CDCl_3$ as solvent and tetramethylsilane (TMS) as internal standard. Elemental analysis was performed with a PE-2400 II elemental apparatus. Differential scanning calorimetry (DSC) was performed using a Pyris Diamond DSC system at a scan rate of 10 □ min^{-1} through a heating-cooling-heating cycle. The liquid crystalline textures were observed on a polarizing optical microscope (Olympus, BX51) equipped with a hot stage (Linklam TMS 94) by cooling the compounds from isotropic phase to liquid crystalline phase. Infrared spectra were measured on the KBr pellets of the samples using a Perkin-Elmer Spectrum 2000 FTIR

spectrometer with a high-temperature attachment. Each sample was heated at a rate of 10 ºC min^{-1} and was kept for 5 min at the selected temperature prior to scanning. XRD analysis was performed using a Rigaku D/MAX-RC X-ray powder diffractometer with Cu Ka radiation (k = 1.5408) at room temperature and elevated temperatures. The samples were tested at the selected temperatures under vacuum. Each sample was heated at a rate of 10 ºC min^{-1} and kept for 5 min at the selected temperature prior to scanning. Data were recorded from 2 to 30º in steps of 0.03º. CD spectra were recorded on a circular dichroism (Applied Photophysics Chirascan) spectropolarimeter using ethanol as solvent.

Results and Discussion

D- and L-C_nACS were prepared by direct salt formation reactions. **Figure 1** shows the ^{1}H NMR spectra of D-C_{12}ACS and D-CSA and peak assignments. The chemical shifts of the H atoms on the CSA ring were altered slightly towards the high field after salt formation and new peaks corresponding to the H atoms of dodecylamine appeared. Elemental analysis of D-C_{12}ACS was also determined, (%); Calcd: C(63.31), N(3.36), S(7.67); Found: C(63.56), N(3.30), S(7.45). The ^{1}H NMR chemical shifts and elemental analysis results of D- and L-C_nACS are listed in **Table 1**, which are in agreement with their structures.

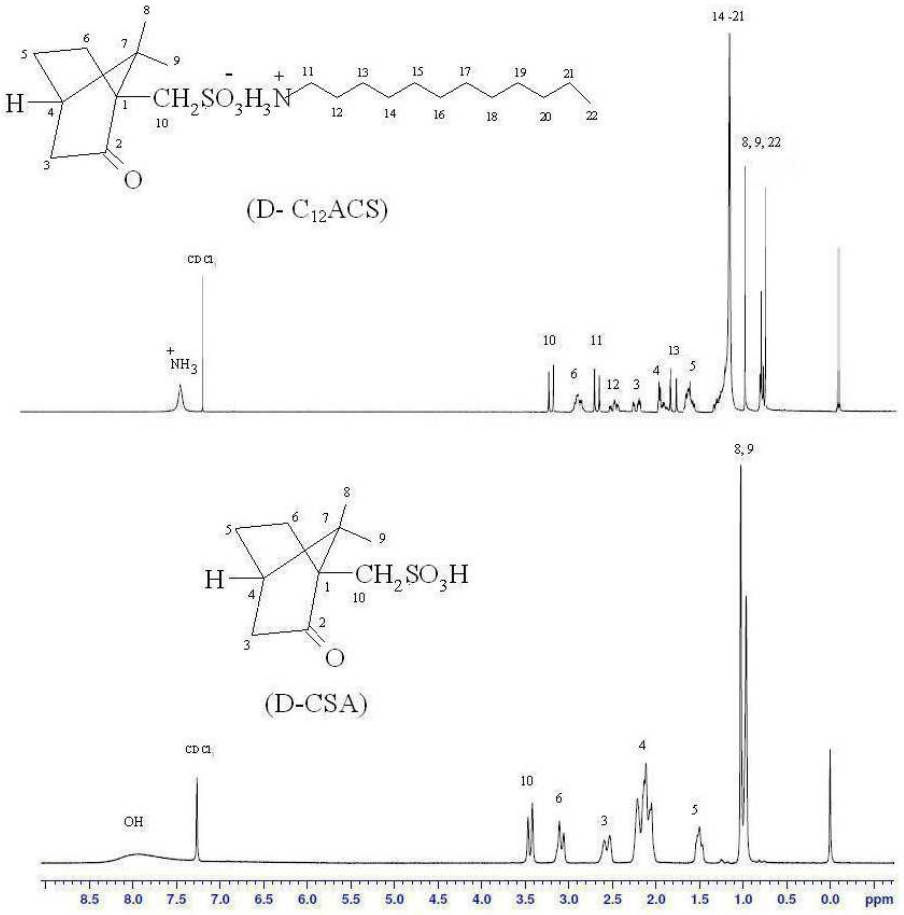

Figure 1. ^{1}H-NMR spectra of D- C_{12}ACS and D-CSA

Table 1. ^{1}H NMR chemical shifts (δ) of D- and L-C_nACS

ILCs	H^{3}	H^{4}	H^{5}	H^{6}	$H^{8,9}$	H^{10}	H^{11}	H^{12}	H^{13}	$H^{14,*}$
D-CSA	2.59	2.21	1.52	3.11	1.02	3.47	-	-	-	-
D-C_{12}ACS	2.28	2.06	1.68	2.99	1.25	3.30	2.80	2.60	1.91	1.35
D-C_{14}ACS	2.30	2.06	1.67	2.98	1.25	3.30	2.80	2.60	1.92	1.37
D-C_{16}ACS	2.30	2.05	1.70	2.99	1.25	3.31	2.81	2.60	1.92	1.37
D-C_{18}ACS	2.30	2.06	1.71	2.99	1.06	3.31	2.80	2.60	1.92	1.35

L-C_{12}ACS	2.28	2.07	1.69	2.99	1.25	3.31	2.76	2.60	1.92	1.35
L-C_{14}ACS	2.29	2.07	1.74	2.99	1.25	3.31	2.80	2.60	1.92	1.36
L-C_{16}ACS	2.30	2.07	1.73	2.98	1.06	3.30	2.81	2.54	1.92	1.30
L-C_{18}ACS	2.30	2.06	1.71	3.00	1.06	3.30	2.80	2.60	1.92	1.30

*: CH_2 groups of long alkyl chains

D- and L-C_nACS were subjected to a heating-cooling-heating scan cycle at a rate of 10 ºC min^{-1} in DSC analysis. Liquid crystal behavior was noted for all D- and L-isomers. **Figure 2** shows the typical DSC traces of D-C_{12}ACS between 0 and 140 ºC. Two endothermic peaks appeared at 41.6 ºC with an enthalpy change of 29.2 J g^{-1} and at 127.5 ºC with an enthalpy change of 43.3 J g^{-1} in the first heating, respectively. These two peaks corresponded to the crystal-to-mesophase transition and mesophase-to-isotropic transition, respectively. Thermogravimetric analysis (TGA) indicated that the samples were stable in the temperature range of the DSC experiments, because no mass losses were noted below 200 ºC in the TGA experiments of these samples (**Figure S1**). The TGA result suggested that residual solvent was not likely to present in the samples, therefore, these two DSC peaks were not due to the intercalation phenomenon caused by solvent.[28] The mesophases were smectic and were identified as smectic B* (SmB*) phases by the XRD and CD measurements as described in the folowing sections. Temperature hysteresis was observed by comparing the cooling and heating curves. In the first cooling process, the sharp peak associated with the transition from isotropic melt to liquid crystal was 34 ºC lower than that in the first heating trace. Generally, the lower melting temperatures found at the second heating trace can be explained by the

occurrence of smaller crystal sizes after crystallization during the first cooling from the melt.[29] In the second heating process, the peak associated with the crystalline-to-smectic transition became flat compared with the corresponding sharp peak in the first heating. This result implies the heating of optically active compounds at high temperatures induced racemization.[24] Therefore, special care must be taken to avoid unnecessarily prolonged heating at high temperatures for optical active compounds.[24]

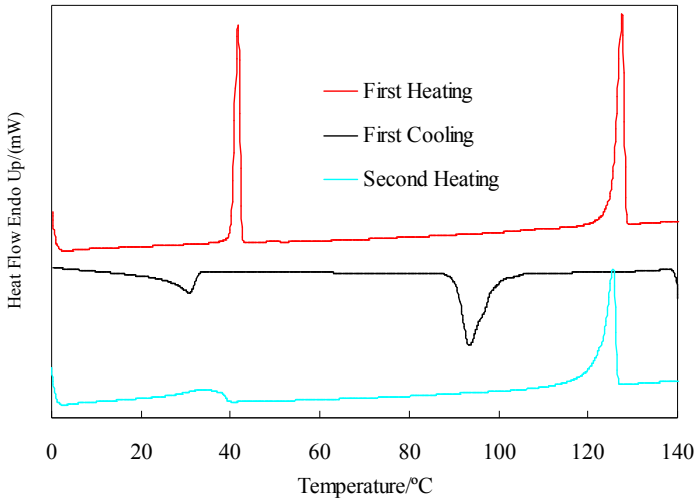

Figure 2. DSC traces of D-C_{12}ACS run from 0 to 140 ºC at a scan rate of 10 ºC min^{-1}.

Table 2 gives the phase transition temperatures, transition enthalpies and mesophase ranges of for D- and L-C_nACS determined from the first heating. The dodecylammonium salts of D- and L-camphorsulfonic acids had low transition temperatures at 41.6 and 41.8 ºC at the first heating, and 34.3 and 34.0 ºC at the second heating, respectively. The mesophase ranges for D-C_{12}ACS, D-C_{14}ACS, D- C_{16}ACS and D-C_{18}ACS were 85.9, 57.0, 54.8 and 47.0 ºC, respectively, according to the first heating process. The salts with

shorter alkyl chain lengths exhibited lower transition temperatures from crystal to liquid crystal phase with wider mesophase ranges, which was contrary to that of the salts with a smaller five-membered pyroglutamic acid rigid core.[24] It is also essential to note that there was a clear increase in crystal-liquid crystal phase transition temperature with increase in the alkyl chain length (n), indicating that more stable crystal structure occurred in the crystalline phase with incrasing alkyl chain length. However, the melting tempareature of the liquid crystal-isotropic phase transition only increased slightly with chain length, indicating the chain length had a minimum influence on the clearing process. This behavior suggests that the crystal stability of the compound was mainly controlled by the packing of the alkyl chains; however, the smectic phase stability was dominated instead by the packing of bulky rigid camphorsulfonic acid core.

Table 2. Transition temperatures (T) and transition enthalpies (ΔH) and mesophase ranges (ΔT) of D- and L-C_nACS

ILCs	$T_{(Cr^*- SmB^*)}$/°C	$\Delta H_{(Cr^*-SmB^*)}$/J g^{-1}	$T_{(SmB^* -I^*)}$/°C	$\Delta H_{(SmB^* -I^*)}$/J g^{-1}	ΔT/°C[a]
D-C_{12}ACS	41.6	29.2	127.5	43.3	85.9
D-C_{14}ACS	62.9	52.5	119.9	36.2	57.0
D-C_{16}ACS	68.7	56.3	123.5	32.9	54.8
D-C_{18}ACS	79.3	71.6	126.3	36.0	47.0
L-C_{12}ACS	41.8	29.7	128.4	45.2	86.6
L-C_{14}ACS	60.7	40.1	126.4	44.8	65.7
L-C_{16}ACS	72.5	52.8	123.1	33.5	50.6

L-C_{18}ACS	78.7	73.8	123.0	37.7	44.3

Cr*: chiral crystal phase; SmB*: chiral smectic B* phase; I*: chiral isotropic liquid, a: $\Delta T = T_{(SmB^*-I^*)} - T_{(Cr^*-SmB^*)}$

When a polarized light source passes through a liquid crystal, a specific textures which reflects the presence of some ordered domains in the material can be observed. The liquid crystal textures of the D- and L-C_nACS were investigated using a by polarized optical microscope. **Figure 3** shows the POM textures of some D and L-C_nACS at liquid crystal phase at 80 ºC. Upon cooling the compound from isotropic melt to liquid crystal phase, well-developed textures were observed, suggesting the presence of the smectic liquid crystal phases.

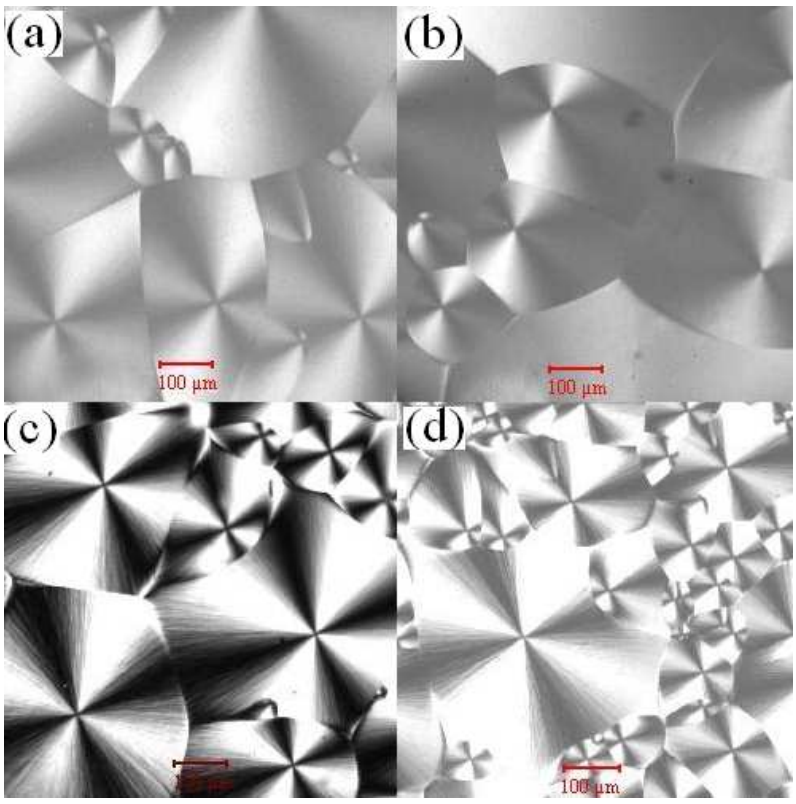

Figure 3. POM images of liquid crystals at 80 ºC: (a) L-C_{12}ACS; (b) D-C_{14}ACS; (c) L-

C_{16}ACS, and (d) D-C_{18}ACS.

Figure 4 shows the FTIR spectra of L-C_nACS at different temperatures. At room temperature when the materials were in the crystalline state, a strong and broad peak around 3450 cm^{-1} which was attributed to the stretch of the bonded N-H in the ammonium group was present in the spectra. However, the intensity of the bands at 3450 cm^{-1} substantially decreased with increasing teperature. When the temperature was raised to 90 ºC, the compounds were well transformed into their corresponding liquid crystalline state and the band at 3450 cm^{-1} almost completely disappeared. The intensity of IR absorption is determined by the magnitude of the transition probability and the change of dipole moment. When the temperature was increased, the expansion of the surrounding crystal structures caused the decrease of the electron density of the H atoms and thus the change of dipole moment, resulting in decrease in the integral absorption coefficient change.[30] It was also noted that the bands at 3450 cm^{-1} became weaker with increasing alkyl chain length, suggesting the the hydrogen bonding btween neiboring moleculaes was weaken too with increasing alkyl chain length. D-C_nACSs exhibited the similar FTIR spectra as their L-C_nACS counterparts (**Figure S2**).

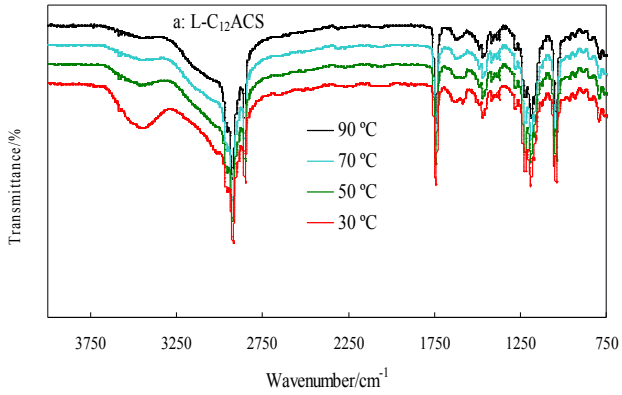

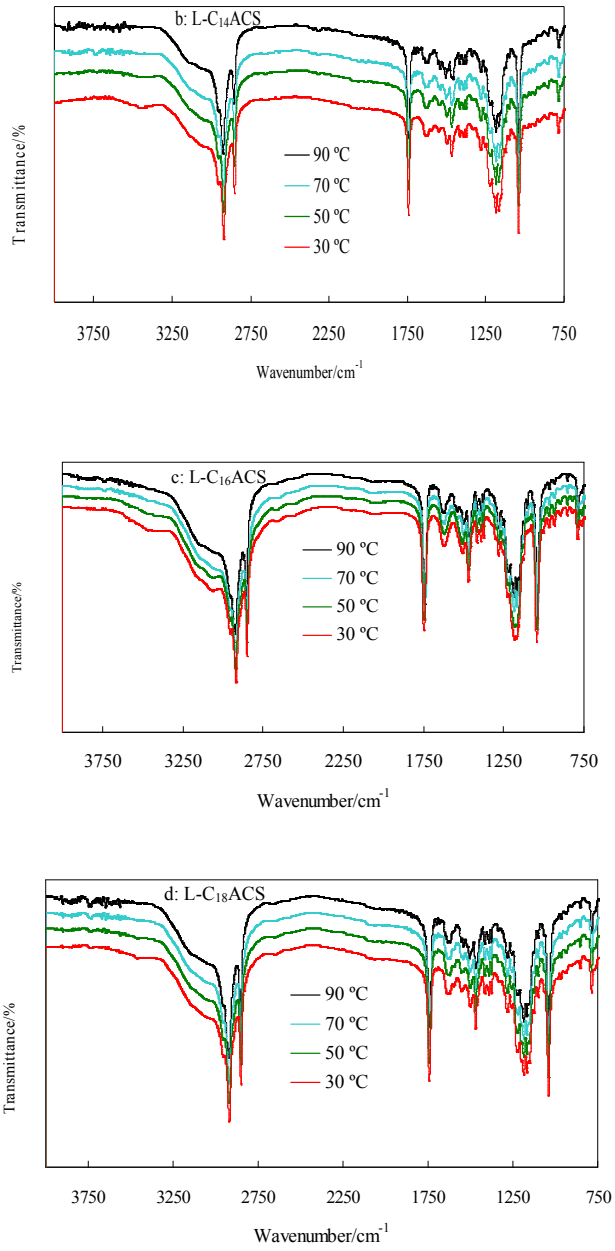

Figure 4. FTIR spectra of (a) L-C_{12}ACS, (b) L-C_{14}ACS, (c) L-C_{16}ACS and (d) L-C_{18}ACS at different temperatures.

Variable temperature X-ray diffraction was performed to gain more details on the molecular arrangements in solid state and liquid crystalline phases. **Figure 5** shows the XRD

patterns of L-C_nACS at room temperature (RT) and 90 ºC. The X-ray patterns of the salts with 16 and 18-carbon chains exhibited many sharp Bragg reflections located both at small and wide angles in the crystal phases, showing the existence of well-developed three-dimensional crystal packing of the molecules.[31] However, the salts with 12 and 14-carbon chains exhibited a less peaks at wide angles, indicating of more extended orientation compared with longer chain salts. In the liquid crystal state, many refractions were weakened or disappeared except a strong small-angle diffraction peak corresponding to the layer spacing, indicating the molecules had more extended orientation in the liquid crystal phase than in the crystal phase. D-C_nACS exhibited the similar XRD patterns as their L-C_nACS counterparts (**Figure S3**).

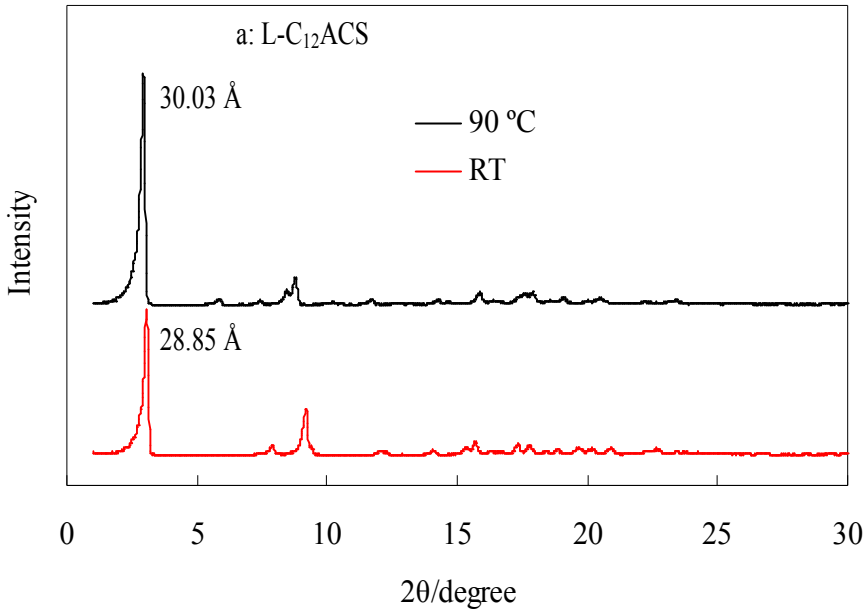

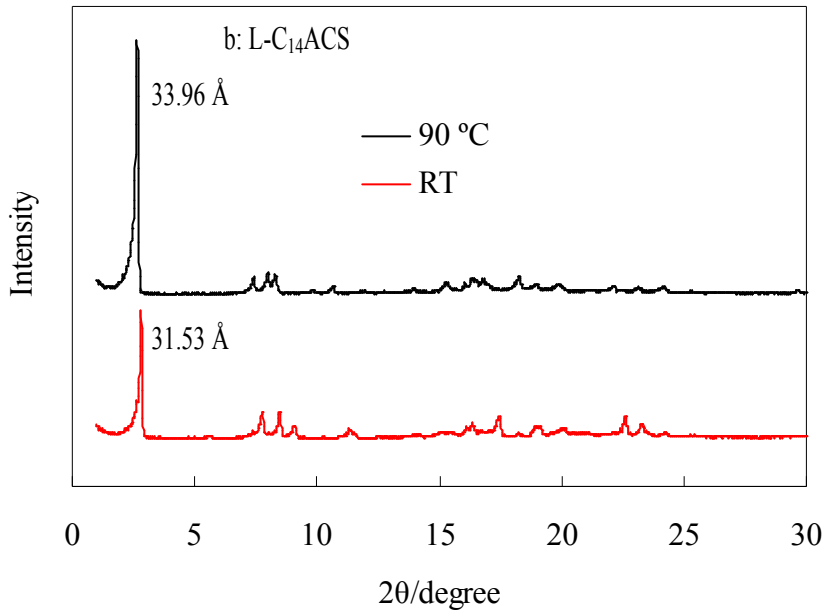

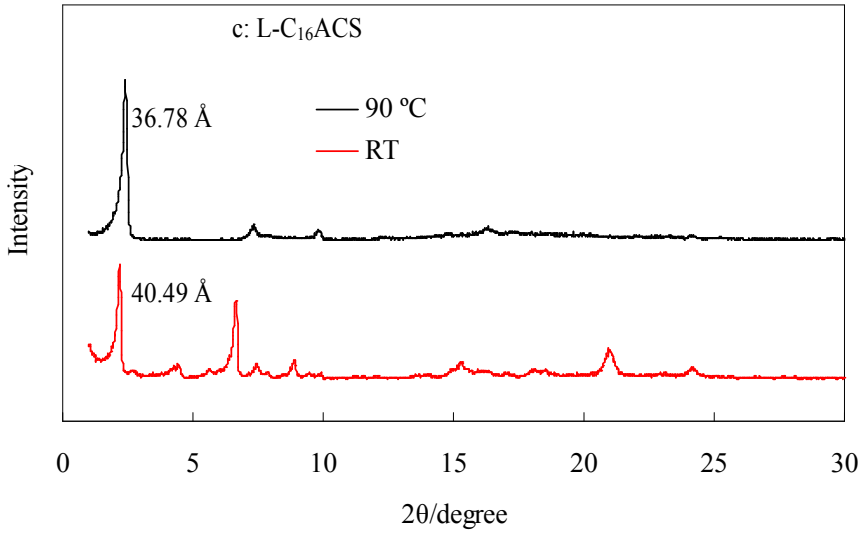

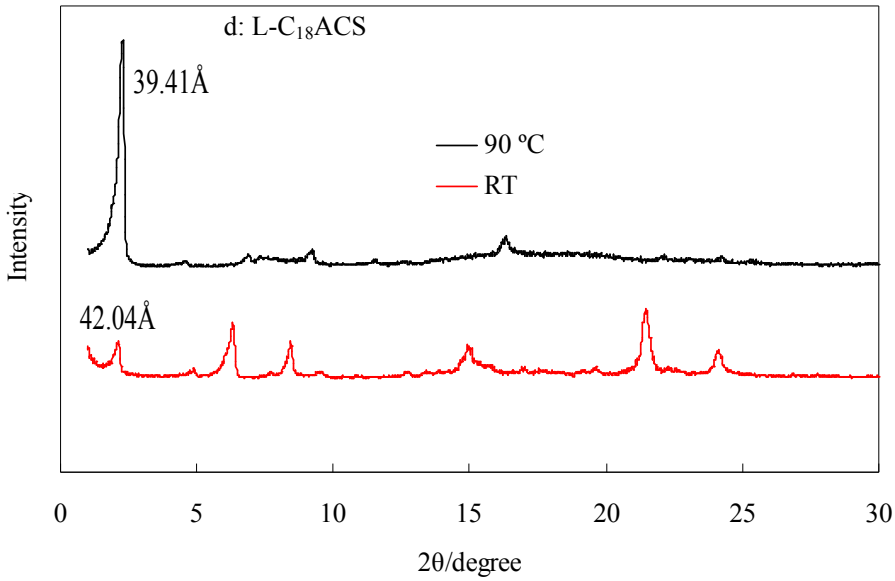

Figure 5. X-Ray diffraction patterns of (a) L-C_{12}ACS, (b) L-C_{14}ACS, (c) L-C_{16}ACS and (d) L-C_{18}ACS at room temperature and 90 °C.

The XRD patterns of D- and L-C_nACS in the mesophase exhibits a sharp peak at small angle and a peak near 16.4º in 2θ. This RXRD pattern was consistent with that of a SmB phase.[32] Because these D- and L-C_nACS compounds are chiral, their liquid crystal phases are expected to be smectic B* phases. The layer spacing of each compound at different temperatures, which was calculated from the 001 line, are listed in **Table 3**. The layer spacing (d) of the salts increased upon transition from crystal state to mesophase when the chain carbon numbers were 12 and 14. This increase was probably caused by the alignment of the molecular rod perpendicular to the layer plane, which tended to elongate the layer spacing. However, when the chain carbon numbers were 16 and 18, the d spacing of the salts decreased upon transition from crystalline phase to mesophase. This was probably because at elevated temperatures the longer chains exhibited large propensity to bend under the

influnecy of thermal motion of the chains, leading to the reduction in layer spacing of the mesophase.

Table 3. The layer spacing (d) and increment of layer spacing (Δd) of D- and L-C_nACSs

ILCs	$d_{(Cr^*)}$/Å	$\Delta d_{(Cr^*)}$/Å [a]	$d_{(SmB^*)}$/Å	$\Delta d_{(SmB^*)}$/Å [b]
D-C_{12}ACS	29.04	-	30.44	-
D-C_{14}ACS	31.98	2.94	34.22	3.78
D-C_{16}ACS	40.12	8.14	36.78	2.56
D-C_{18}ACS	43.06	2.94	40.49	3.71
L-C_{12}ACS	28.85	-	30.03	-
L-C_{14}ACS	31.53	2.68	33.69	3.66
L-C_{16}ACS	40.49	8.96	36.78	3.09
L-C_{18}ACS	42.04	1.55	39.41	2.63

Cr*: chiral crystal phase (room temperature); SmB*: chiral smectic B* phase (T =90 ºC);
[a]: change of layer spacing in crystal phase with an increase of 2 carbons in chain length;
[b]: change of layer spacing in liquid crystal phase with an increase of 2 carbons in chain length.

In the crystalline state, the layer spacing for D- and L-C_nACS with chain lengths of 12 and 14 carbons were at the same level. On the other hand, the D- and L-C_nACS with chains of 16 and 18 carbons exhibited similar layer spacing. However, D- or L-C_nACS experienced a large change in layer spacing (Δd) when the alkyl chain length increased from 14 to 16 carbons, being 8.14, and 8.96 Å (**Table 3**), respectively, indicating the salts with chains of 12 and 14 carbons had different arrangements from the salts with chains of 16 and 18 carbons.

This difference in chain arrangement of the layers was also reflected in the XRD patterns which showed the salts with 16 and 18 carbon chains had more bragg's diffractions. In the smectic B* phase at 90 ºC, the Δd of D- and L-C_nACS from 12 to 14, 14 to 16 and 16 to 18 were 3.78, 2.56, 3.71 and 3.66, 3.09, 2.63 Å, respectively. As shown in **Table 3**, with increase in chain length, the layer distances of salts showed an increasing trend for both crystalline and liquid crystal phases at room temperature. This result indicates the layer distance at the liquid crystal phase increased approximately linearly with the increment of chain length. However, the layer distance of the salts at the crystal phase displayed a robust increase when the chain length increased from 14 to 16 carbons, which was contrary to the linear increment displayed by the salts with straight chains of 12 to 18 carbons [10] and a smaller five-membered pyroglutamic acid rigid core [24] at crystal and liquid crystal phases. This result suggested that D- and L-C_nACS exhibited extended arrangements when the chain lengths were short but became bended when the alkyl chains were long.

Circular dichroism (CD) spectrum reveals the chirality of molecule and often provides information on the assembled structures.[33] To confirm the optical activity of D- and L-C_nACS, the CD spectra of D-C_{18}ACS and L-C_{18}ACS in ethanol solution were scanned using a CD spectrometer (**Figure 6).** D-C_{18}ACS exhibited negative cotton effects at *ca*. λ_{max} 210 nm and a positive signal at *ca*. λ_{max} 290 nm, while L-C_{18}ACS displayed an exactly opposite pattern. It was found that D and L compounds had the same CD signal intensities, with opposite signal due to the opposite absolute configuration at the chiral center. The CD signals mean that chiral center existed in D- and L-C_nACS.

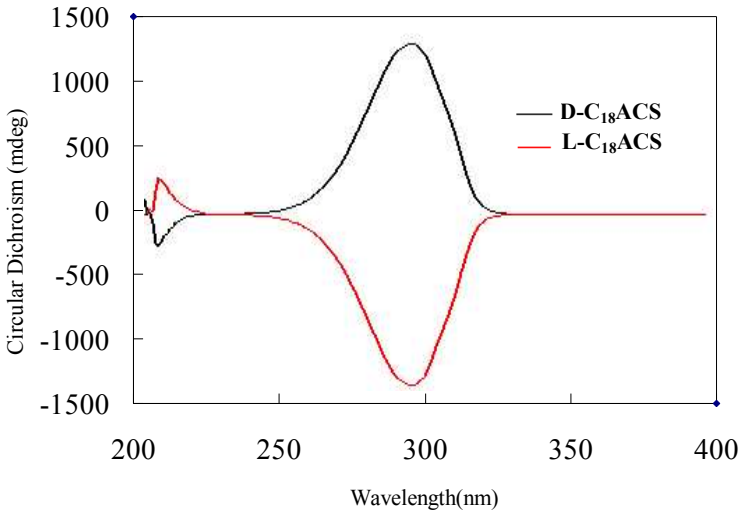

Figure 6. CD spectra of D-C_{18}ACS and L-C_{18}ACS.

Conclusions

Alkylammonium champhorsulfonates were prepared and exhibited ionic liquid crystalline behaviors. The ILC salts with shorter chains exhibited lower crystal-to-liquid crystal transition temperatures and wider mesophase ranges. The vibration of N-H bond were weakened or disappeared at the SmB* phase, which were caused by the change of dipole moment of the liquid crystals and constrained of N-H bond in the SmB* phase. The layer spacing (d) increase upon transition from crystal to mesophase when the chain numbers were 12 and 14, possibly as a result of the alignment of the molecular rod perpendicular to the layer plane. However, the mesophase d spacing decreased upon transition from crystal to mesophase when the chain carbon numbers were 16 and 18, which was probably because the thermal motion of the chains at the mesophase tended to shorten the layer spacing. Layer distance for the salts at liquid crystal phase increased with the increment of chain length. However, the layer distances of the salts in the

crystalline phase showed a robust increase when the chain length increased from 14 to 16 carbons, indicating that the the alkyl chain bended to a degree when they were long.

Acknowledgements

This research was supported by the grants from National Natural Science Foundation of China (Project No. U1202265); Institute of the Chinese Academy of Forestry, Fundamental Research Foundation of the Central Commonwealth (Project No. CAFYBB2012038); and Chinese Scholarship Council (201203270006). The authors are also grateful for the technical support and facilities provided by the Composite Materials and Engineering Center at Washington State University.

References

1 C. Tschierske, *J. Mater. Chem.*, 2001, **11,** 2647-2671.

2 M. Yoshio, T. Kagata, K. Hoshino, T. Mukai, H. Ohno and T. Kato, *J. Am. Chem. Soc.*, 2006, **128,** 5570-5577.

3 K. Goossens, K. Lava, P. Nockemann, K. Van Hecke, L. Van Meervelt, P. Pattison, K. Binnemans and T. Cardinaels, *Langmuir*, 2009, **25,** 5881-5897.

4 N. V. Madhusudana, *Curr. Sci.*, 2001, **80,** 1018-1025.

5 K. Binnemans, *Chem. Rev.*, 2005, **105,** 4148-4204.

6 J. S. Wilkes, *Green Chem.*, 2002, **4,** 73-80.

7 T. Welton, *Chem. Rev.*, 1999, **99,** 2071-2084.

8 R. Sheldon, *Chem. Commun.*, 2001, 2399-2407.

9 P. Wasserscheid and W. Keim, *Angew. Chem., Int. Ed.*, 2000, **39,** 3772-3789.

10 M. Arkas, D. Tsiourvas, C. M. Paleosand and A. Skoulios, *Chem. Eur. J.*, 1999, **5,** 3202-3207.

11 R. Martin-Rapun, M. Marcos, A. Omenat, J. Barbera, P. Romero and J. L. Serrano, *J. Am. Chem.Soc.*, 2005, **127,** 7397-7403.

12 M. Marcos, R. Alcala, J. Barbera, P. Romero, C. Sanchez and J. L. Serrano, *Chem. Mater.*, 2008, **20,** 5209-5217.

13 A. E. Bradley, C. Hardacre, J. D. Holbrey, S. Johnston, S. E. J. McMath and M. Nieuwenhuyzen, *Chem. Mater.*, 2002, **14,** 629-635.

14 W. Dobbs, L. Douce, L. Allouche, A. Louati, F. Malboscand and R. Welter, *New J. Chem.*, 2006, **30,** 528-532.

15 K. Goossens, K. Lava, P. Nockemann, K. V. Hecke, L. V. Meervelt, K. Driesen, C. Gorller-Walrand, K. Binnemans and T. Cardinael, *Chem. Eur. J.*, 2009, **15,** 656-674.

16 J. Y. Z. Chiou, J. N. Chen, J. S. Lei and I. J. B. Lin, *J. Mater. Chem.*, 2006, **16,** 2972-2977.

17 F. Reinitzer, *Monatsh. Chem.*, 1888, **9,** 421-441.

18 J. W. Goodby, I. M. Saez, S. J. Cowling, V. Gortz, M. Draper, A. W. Hall, S. Sia, G. Cosquer, S. E. Lee and E. Peter Raynes, *Angew. Chem., Int. Ed.*, 2008, **47,** 2754-2787.

19 H. T. Nguyen, M. Ismaili, N. Isaertb and M. F.Achard, *J. Mater. Chem.*, 2004, **14,** 1560-1566.

20 J. F. Li, J. J. Stott, E. A. Shack, X.Y. Wang, R. G. Petschek and C. Rosenblatt, *Liq. Cryst.*, 1997, **23,** 255-261.

21 T. Kato and J. M. J. Frechet, *J. Am. Chem. Soc.*, 1989, **111,** 8533-8534.

22 F. C. Yu and L. J. Yu, *Chem. Mater.*, 2006, **18,** 5410-5420.

23 Matsunaga, Y.; Tsujimura, T. *Mol. Cryst. Liq. Cryst.* **1991**, *200*, 103.

24 D. Tsiourvas, C. M. Paleos and A. Skoulios, *Chem. Eur. J.*, 2003, **9,** 5250-5258.

25 Tsiourvas, D.; Mihou, A. P.; Couladouros, E. A.; Paleos, C. M. *Mol. Cryst. Liq. Cryst.* **2001**, *362*, 177.

26 P. D. Bartlett and L. H. Knox, *Org. Synth.*, 1973, **5,** 194-195.

27 Y. Cao, P. Smith. *Polymer*, 1993, **34**, 3139-3143.

28 A. Mujahid, H. Stathopulos, P.A. Lieberzeit, F.L. Dickert, *Sensors,* 2010, **10** , 4887-4897.

29 A. F. Theunemann, D. G. Kurth, M. Beinhoff, R. Bienert and B. Schulz, *Langmuir*, 2006, **22,** 5856-5861.

30 Y. Yand, M. Feng, P. Zhang, *Am. Mineral.*, 2010, **95**, 1439 - 1443.

31 M. Sikiric, I. Smit, L. Tusek-Bozic, V. Tomasic, I. Pucic, I. Primozic and N. Filipovic-Vincekovic, *Langmuir*, 2003, **19,** 10044-10053.

32 M. Stojanovic, A. Bubnov, D. Z. Obadovi, V. Hamplov, M. Kaspar, M. Cvetinov *Phase Transit.,* 2011, ***84***, 380-390.

33 G. Gottarelli, S. Lena, S. Masiero, S. Pieraccini and G. P. Spada, *Chirality*, 2008, **20,** 471-485.

Chiral ionic liquid crystals with a bulky rigid core from renewable camphorsulfonic acid

Xiaoping Rao, Jinwen Zhang, Jianqiang Zheng, Zhanqian Song and Shibin Shang

Renewable chiral D- and L-camphorsulfonic acids were introduced as new building blocks for the design of ionic liquid crystals.